International Journal of ChemTech Research
CODEN(USA): IJCRGG ISSN : 0974-4290
Vol.6, No.2, pp 1070-1080, April-June 2014

Growth and Characterization of Pure and Metal doped Sodium Sulphanilate Dihydrate (SSDH) single crystals

M. Anantharaja, P. Sathya and R. Gopalakrishnan*

Crystal Research Lab, Department of Physics, Anna University, Chennai – 600025, India.

***Corres. author: krgkrishnan@annauniv.edu, krgkrishnan@yahoo.com**
Tel: +91-44-2235 8710 / 8707; Fax: +91-44-22358700

Abstract: Good quality single crystals of pure and metal doped Sodium Sulphanilate Dihydrate (SSDH) single crystals were grown from aqueous solution by employing slow evaporation solution growth technique. Structural characterization of the grown pure and metal doped SSDH single crystals was carried out by single crystal and powder X-ray diffraction analysis. The functional groups present in the grown crystals were ascertained using FTIR spectroscopic analysis. The UV-Vis spectral studies enumerated that the doping has enhanced the optical transparency of the doped SSDH crystals. Mechanical strength of the grown pure and doped SSDH crystals were analyzed by Vickers microhardness tester. EDAX spectrum revealed that with increasing percentage doping, the grain size had increased. Growth habits were significantly influenced and modified due to doping. The various investigations indicate the changes in structural, optical and mechanical properties of the doped SSDH crystals due to the incorporation of the metal dopant into the SSDH crystal lattice.

Keywords: Optical property, High-resolution X-ray diffraction, Microhardness, Dielectric properties, Growth from solutions, Doping.

Introduction

Single crystals are the backbone of the modern technological revolution. The impact of single crystals is clearly visible in industries like semiconductor, optics, etc. With the invention of lasers, the field of nonlinear optics touched new heights and practical implementation was also possible with the application of nonlinear optical crystals [1-3]. Now-a-days great attention has been devoted to the growth and characterization of pure and metal doped SSDH crystals with the aim of identifying new materials for practical purposes. The effect of dopants on various properties of single crystals is of great interest from both solid state science as well as technological point of view [4]. Additions of dopants have a profound influence on the growth kinetics, morphology and second harmonic efficiency of SSDH crystals. The pure and doped SSDH single crystal grown by slow evaporation solution growth method. But in the literature survey, to the best of our knowledge, there is no report on the systematic growth and characterization of zinc and cadmium metals doped with SSDH crystals[5]. The grown crystals were characterized by X-ray diffraction technique, EDAX study, FTIR analysis, TGA/DTA, microhardness and Dielectric studies.

1. Experimental Procedure

1.1 Crystal Growth

Single crystals of pure and doped SSDH were grown by solution growth method by employing slow evaporation technique at room temperature. Sodium sulphanilate dihydrate was synthesized using sulfanilic acid and sodium carbonate from Merck (GR-grade) in the stoichiometric ratio 2:1 in double distilled water. The reactants were thoroughly dissolved indouble distilled water and stirred well for an hour to yield a homogeneous mixture of solution which was prepared in accordance with the solubility data. The beaker containing the saturated solution (50 ml) was closed with perforated cover and kept in a dust free atmosphere to allow slow evaporation of the solvent. Transparent, good quality SSDH crystals were harvested within 40 days. For the growth of zinc and cadmium metal doped SSDH crystals, the pure SSDH salts were dissolved in deionized water and 3 % of zinc, cadmium metal were added separately as dopants and mixed thoroughly using a magnetic stirrer and the white crystalline salt of metal doped SSDH was obtained. From the saturated aqueous solution small transparent colorless single crystals of metal doped SSDH were obtained with 20 days by employing slow evaporation technique at room temperature. These crystals were further purified by recrystallization for further growth. The grown pure and metal doped SSDH grown crystals are shown in figure.1.1 (a, b, c and d).

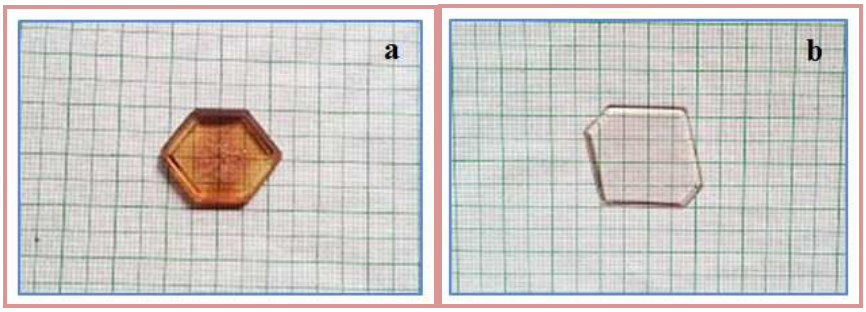

Figure 1.1 (a) Sodium Sulphanilate Dihydrate (SSDH)
(b) Li_2SO_4 doped with SSDH

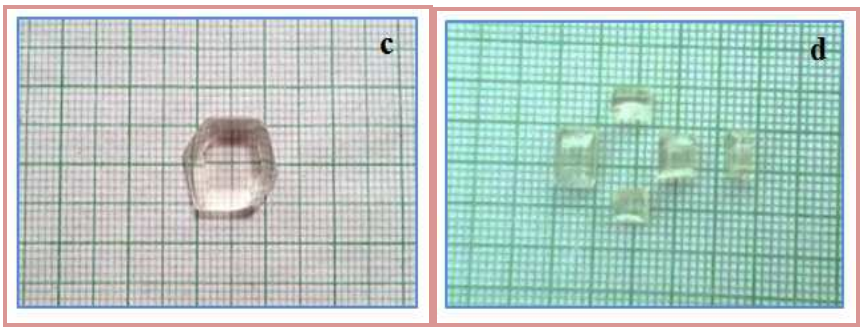

Figure 1.1 (c) Zn SO_4 doped with SSDH
(d) 3Cd SO_4 doped with SSDH

3.1 Results and Discussion

3.1.1 Single crystal X-ray diffraction studies

The single crystal X-ray diffraction of pure and metal doped SSDH was carried out using ENRAF NONIUS CAD4-F single crystal X-ray diffractometer with CuKα(λ = 0.71703 Å) radiation. The calculated lattice parameter values of the pure and metal doped SSDH single crystals are presented in Table 1. Above study reveals that the crystal belongs to orthorhombic system with space group $\boldsymbol{P_{bca}}$ and the lattice parameters are a = 7.944 (6) Å, b = 10.101 (4) Å, c = 23.895 (5) Å and V = 1917 (1) $Å^3$. The lattice parameters of pure and metal doped SSDH were found to be slightly different from pure SSDH. Owing to the incorporation of zinc and cadmium metals in the crystal lattice. The pure SSDH cell parameter values are in good agreement with the reported values[6].

Table 1 Cell parameters for pure and metal doped SSDH grown crystal

Sample	Cell parameters (Å)			Volume (Å^3)
	a	b	c	
Pure SSDH	**7.944 (2)**	**10.101 (4)**	**23.895 (7)**	**1917 (1)**
3CdSO$_4$ doped SSDH	**7.938 (2)**	**10.080 (2)**	**24.002 (2)**	**1921 (2)**
ZnSO$_4$ doped SSDH	**7.939 (3)**	**10.081 (4)**	**23.967 (8)**	**1918 (1)**
Li$_2$ SO$_4$doped SSDH	**7.942 (2)**	**10.101 (2)**	**23.984 (11)**	**1924 (1)**

3.1.2 Powder X-ray analysis

The lattice parameters of pure SSDH and metal doped SSDH were identified by powder X-ray diffraction technique. The diffractogram of the pure and metal doped SSDH were taken in the range of 2θ which is scanned from 10°- 80°. Powder XRD pattern of pure and metal doped SSDH as shown in figure 1.2.

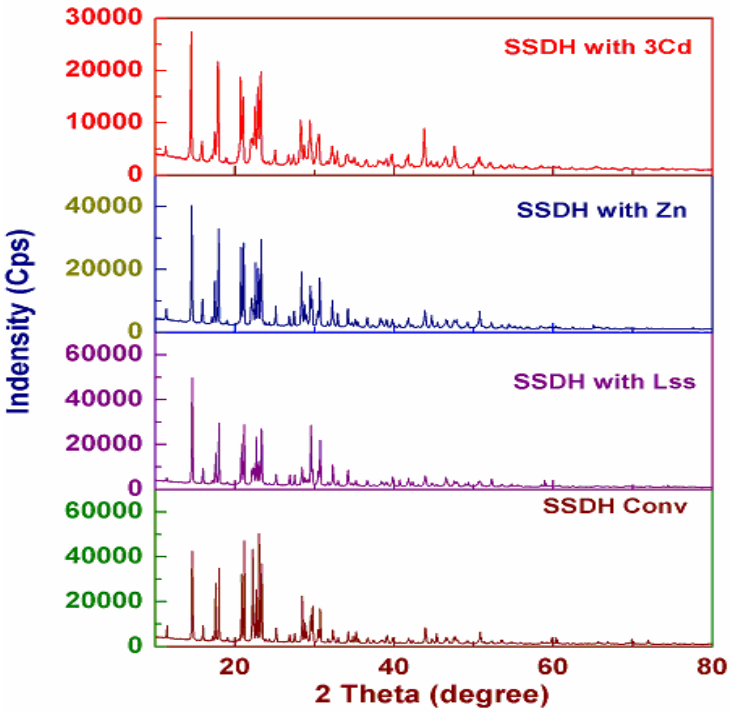

Figure 1.2 Powder XRD pattern of pure and metal doped SSDH grown crystal

3.1.3 Fourier Transform Infrared Spectral Analysis

The influence of the metal dopant SSDH on the vibration frequencies of the functional groups of pure and metal doped SSDH has been identified by FTIR spectroscopy. The FTIR spectra were recorded in the region 500- 4000 cm^{-1} using a Perkin-Elmer RXI spectrometer by KBr pellet technique.

Figure 1.3 shows the FTIR spectra for pure and metal doped SSDH crystals respectively. The interaction and entry of the dopant into the lattice sites of SSDH is clearly indicated by the absent and additional peaks and also by the broadening and shift in the vibrational absorption frequencies of the FTIR spectra. The band observed at 3488 cm^{-1} is due to O-H stretching vibration. The observed broad peak at 3382 cm^{-1} is due to NH stretching. The sharp peak appeared at 3383 cm^{-1} is due to the O-H stretching vibration. The peak at 2150 cm^{-1} is assigned to –C≡C- bending.

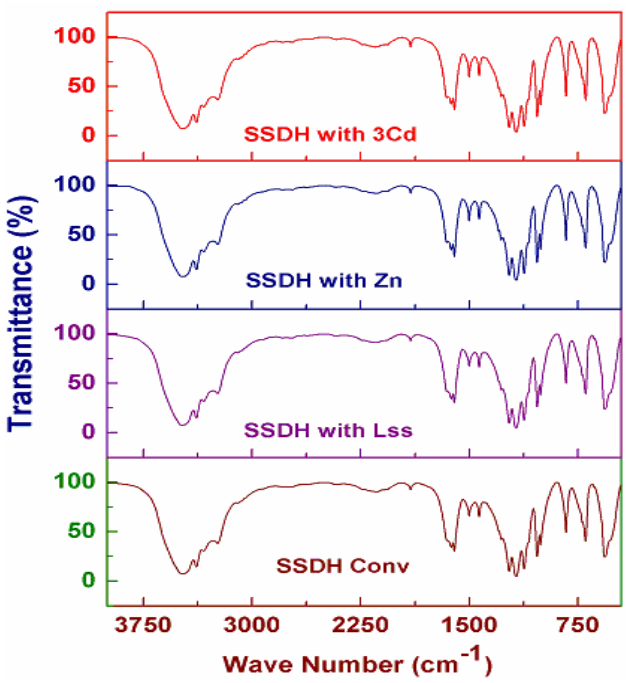

Figure 1.3 FTIR spectrum of pure and metal doped SSDH grown crystal

The sharp peak at 1905 cm^{-1} is due to C-H stretching vibration. TheN-H stretching vibrational frequencies occur at 1657, 1625 and 1603 cm^{-1} and N-O asymmetric stretching vibration occurs at 1431 and 1502 cm^{-1}. The peak at 1225 and 1281 cm^{-1} are assigned due to the stretching modes of C-N of SSDH crystals. The bands observed at 1008, 1033, 1122 and 1175 cm^{-1} correspond to C-O stretching vibration of SSDH. The sharp peak appeared at 834 and 697 cm^{-1} are due to C-H bending mode and the medium band at 568 cm^{-1} corresponds to the C-Br stretching vibration.

3.1.4 Laser Raman spectrum Analysis

The Raman spectrum of pure and doped SSDH was record between 200 and 2000 cm^{-1} alone are presented in the spectrum. The NH proton of SSDH molecule is sufficiently mobile to form strong hydrogen bonding interaction with the neighboring SSDH molecule in the crystal. This interaction may facilitate the centrosymmetric arrangement of SSDH in the crystal lattice. Hence the NH vibration which is reported to have a broad envelopein the IR spectrum is completely absent in this Raman spectrum.

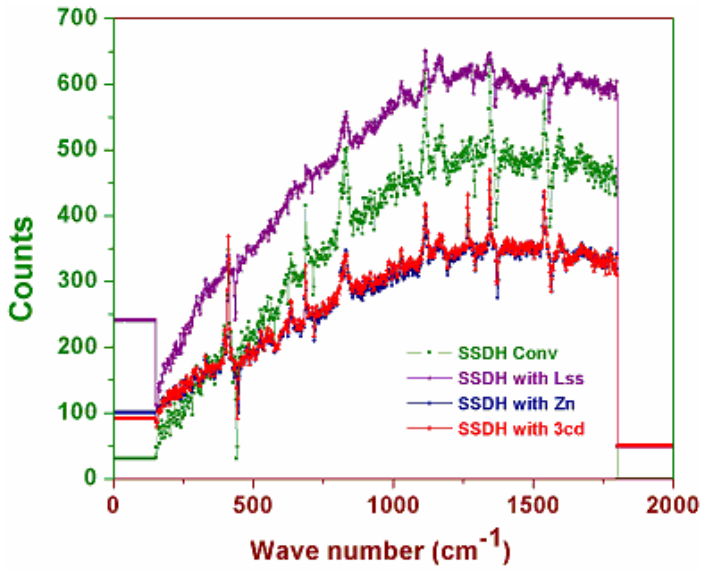

Figure 1.4 Laser Raman spectrum of pure and metal doped SSDH grown crystal

The various vibrations appear between 250 and 1800 cm^{-1} shown in the spectrum. This clearly establishes the more close packed arrangement than that of solution grown crystals. The aromatic ring vibration produced a characteristic peak between 1000 and 1700 cm^{-1}. The laser Raman spectrum of SSDH single crystal is shown in Figure 1.4.

3.2 EDAX analysis

Quantitative EDAX analysis is the most commonly used method for chemical analysis of materials. The elemental analysis was carried out for zinc and cadmium doped SSDH by employing the energy dispersive X-ray analysis (EDAX) technique and the results are shown in figure.1.5 and figure 1.6. This confirmed the weight percentage and the atomic weight percentage of zinc and cadmium present in the crystal lattice are shown in the corresponding tables. The incorporation of the dopant zinc and cadmium in the crystal lattice was confirmed in this analysis. Growth habits are significantly influenced and modified due to doping.

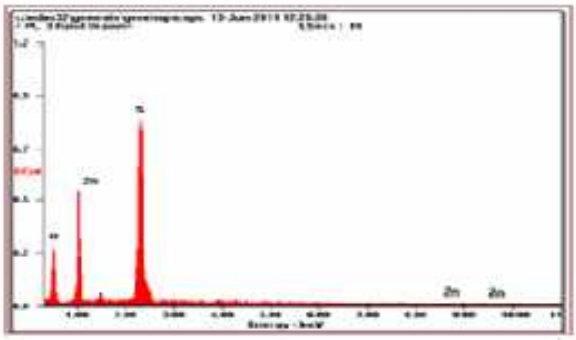

Element	Wt%	At%
OK	59.9	75.17
SK	39.22	24.56
ZnK	0.88	0.27
Matrix	Correction	ZAF

Figure 1.5 EDAX spectrum and data of $ZnSO_4$ doped SSDH grown crystal

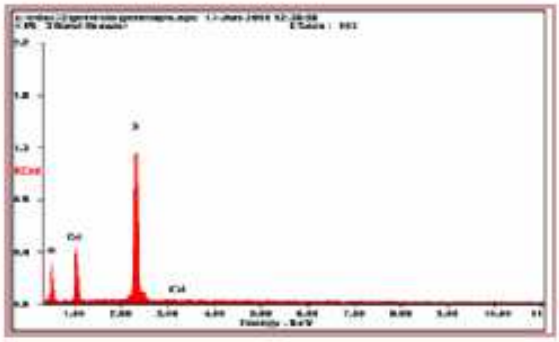

Element	Wt%	At%
OK	55.45	72.07
SK	42.26	27.4
Cd	1.52	0.28
ZnK	0.77	0.25

Figure 1.6 EDAX spectrum and data of $3CdSO_4$ doped SSDH grown crystal

3.3 Optical studies

3.3.1 UV-Vis-NIR Studies

The UV-Visible spectra of the pure and metal doped SSDH crystals were recorded in the wavelength range of 200 - 1100 nm using Perkin Elmer UV-Vis-NIRspectrometer (Model: Lambda 35). Optically polished single crystals of 2 mm thickness were used for the study. It is inferred from the spectra (Figure. 1.7) that both pure and metal doped crystals have large transmission window in the entire visible region, the zinc and cadmium doped SSDH crystal has higher transmittance compared to pure SSDH crystal this is because in the case of metal-organic coordination complexes the organic ligand is more dominant in the NLO and dielectric effects. As for the metallic part, focus is on the group (IIB) metals (Zn, Cd), these compounds usually have higher transparency in UV region, because of their closed d^{10} shells [7,8]. Hence the incorporation of Zn and Cd present in the doped SSDH crystal lattice has progressively improved the crystal quality with higher transparency.

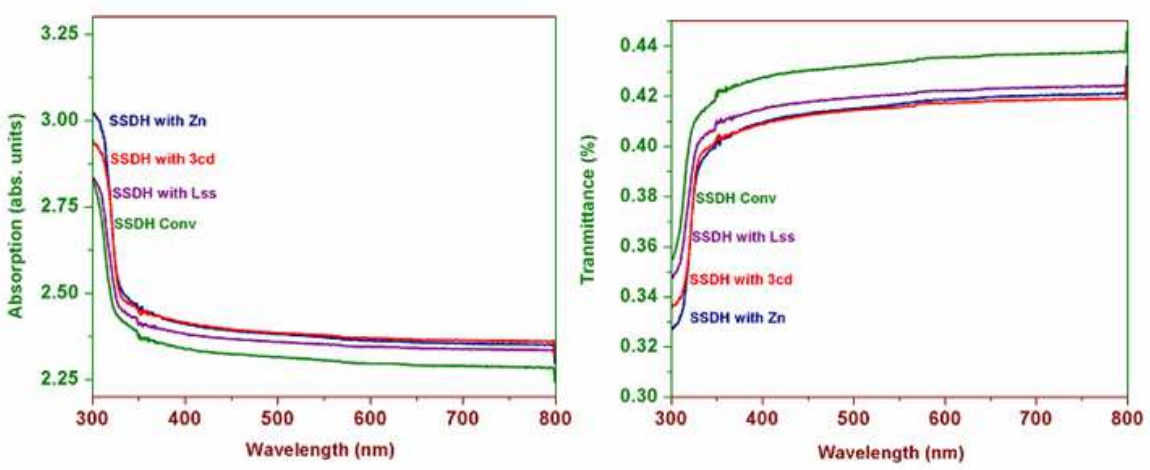

Figure 1.8 UV absorption andTransmission spectrum of pure metal doped SSDH grown crystal

The optical absorption coefficient (α) was calculated from the transmittance using the following relation,

$$\alpha = \frac{2.3036 \log\left(\frac{1}{T}\right)}{d}$$

where T is the transmittance and d is the thickness of the crystal. In the high photon energy region, the energy dependence of absorption coefficient suggests the occurrence of direct band gap. As a direct band gap material, the crystal under study has an absorption coefficient (α) obeying the following relation for high photon energies (hν):

$$\alpha = \frac{A\left(h\upsilon - Eg\right)^{\frac{1}{2}}}{h\upsilon}$$

where Eg is the optical band gap of the crystal, and A is a constant. The variations of $(\alpha h\nu)^2$ versus hν in the fundamental adsorption region were plotted and is shown in Figure. 1.8 and Eg can be evaluated by extrapolation of the linear part[9]. The bandgap is found to be 3.82 eV for conventional grown SSDH single crystal. SSDH doped Lss (3.75 eV), Zn (3.73 eV) and 3Cd (3.73 eV) are respectively. The bandgap decreasing due to the addition of dopens as a consequence of wide band gap, the crystal under study has a large transmittance in the visible region [10]. The band gap of the doped single crystals tends to decrease.

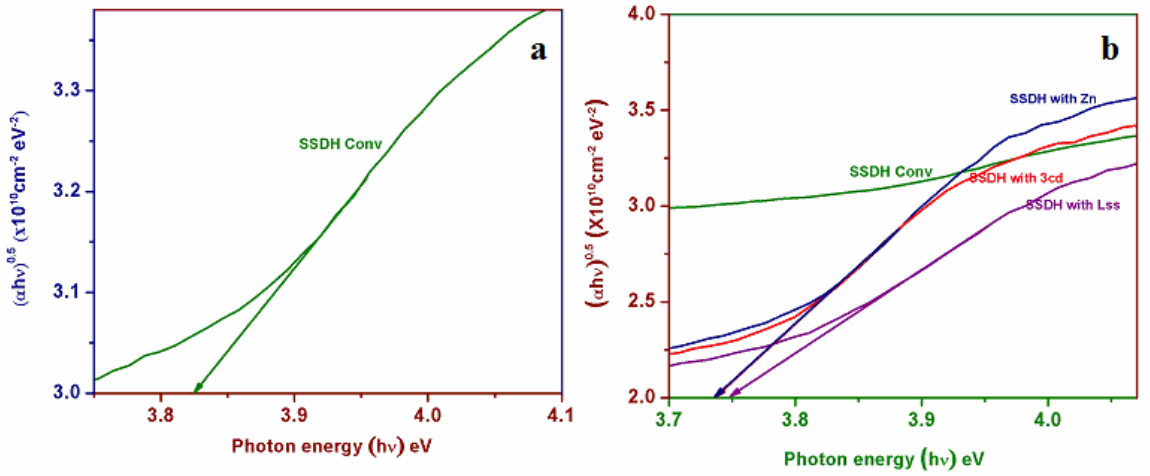

Figure 1.8 Band gap for pure and metal doped SSDH grown crystal

3.3.2 Photoluminescence (PL) studies

The photoluminescence spectroscopy is a nondestructive method of testing used to study in detail the electronic structure of materials[11]. The PL spectrum of the pure and doped crystal SSDH is shown in Figure 1.9.This shows a broad band at 559 nm. The intensity of the peak is low for SPB crystal. The strong yellow emission peak is observed at 561 nm, 566 nm and 572 nm corresponding to the energy of 2.22 eV. The PL intensity is highly dependent on the crystallinity and structural perfection of the crystal. A sharp peak was observed in the range of 300-350 nm in emission spectrum peaking at 561 nm (high intensity peak 85963.0607 a.u). As pure and doped SSDH exhibits similar visible emission at 561 to 572 nm (intensity peaks 29920.84 a.u and 12242 au), the nature of these yellow bands at 2.3eV and 2.2eV can be attributed to radioactive recombination between deep donors and shallow acceptors [12]. The strong PL emission of the title material may find potential applications in optoelectronic devices [13].

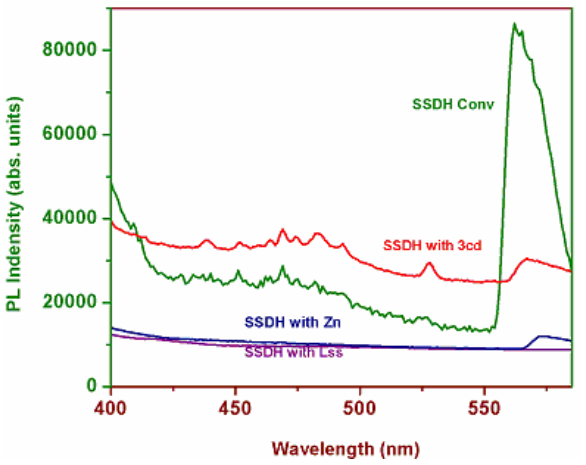

Figure 1.9 PL Spectrum for pure and metal doped SSDH grown crystal

3.4 Vicker's Microhardness analysis

Microhardness testing is taken from the Mmicro – Duromat 4000 E (Reichart - Jung) is one of the best methods of understanding the mechanical properties of materials such as fracture behavior, yield strength, brittleness index and temperature of cracking [14,15]. Hardness of a material is a measure of resistance it offers to local deformation.The pure and doped SSDH crystals were subjected to Vickers Microhardness testing. Vickers Hardness numberH_v was calculated from the following equation:

$$H_v = [(1.8544\ P) / d^2]\ kg/mm^2$$

where P is the applied load in kg and d is the diagonal length of indentation in mm. The plot of Vickers hardness (H_v) versus load (P) for pure and doped SSDH crystals is shown in Figure 1.10. The microhardness value of SSDH crystal was found to be initially increasing with increase of load and then almost constant with further increase of load. The cracks were formed around 90g for all crystals. The subsequent decrease in hardness with increase in load resulted from the activation of cross slip and the movement of piled-up dislocations [16]. The major contribution to hardness is attributed to the high stress required for homogeneous nucleation of dislocation in the small region indented[17], which confirms greater crystalline perfection.

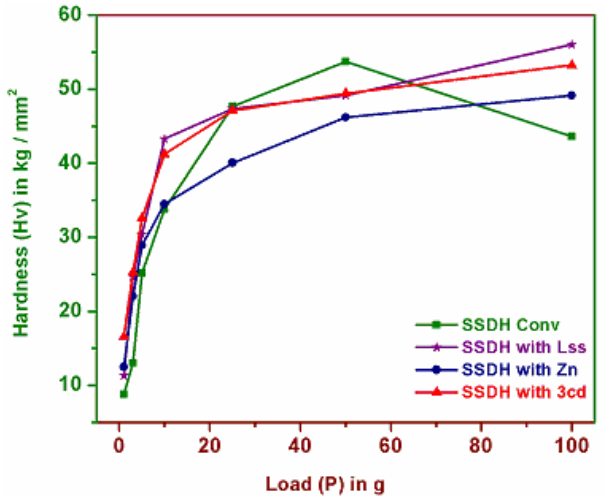

Figure 1.10 Microhardness of pure and metal doped SSDH grown crystal

3.5 Dielectric Studies

Dielectric measurements were performed on a pure and doped SSDH single crystal using a HIOKI HITESTER model 3532-50 LCR meter. The sample of dimensions 2 × 2 × 1 mm^3 has been placed inside a dielectric cell whose capacitance were measured at a temperature of 35°C for different frequencies. The dielectric constant and dielectric loss have been calculated using the equations

$$\varepsilon = \frac{cd}{A\,\varepsilon_0}$$

$$\varepsilon' = \varepsilon \tan \delta$$

where d is the thickness of the sample, A is the area of the sample. The observations are made in the frequency range 50 Hz to 5 MHz at 35°C. Dielectric and loss measurements of optical quality pure and doped SSDH crystal are shown in figure 1.11. From the spectra, it was observed that the dielectric constant and dielectric loss decreases slowly with increasing frequency and attains saturation at higher frequencies. The high dielectric constant of the crystal at low frequency is attributed to space charge polarization [18, 19]. In accordance with Miller rule [20], the lower value of dielectric constant at higher frequencies is a suitable parameter for the enhancement of SHG. The characteristic of low dielectric loss with high frequency for the sample suggests that the crystal possess enhanced optical quality with lesser defects and this parameter play a crucial role for the construction of devices from nonlinear optical materials [21].

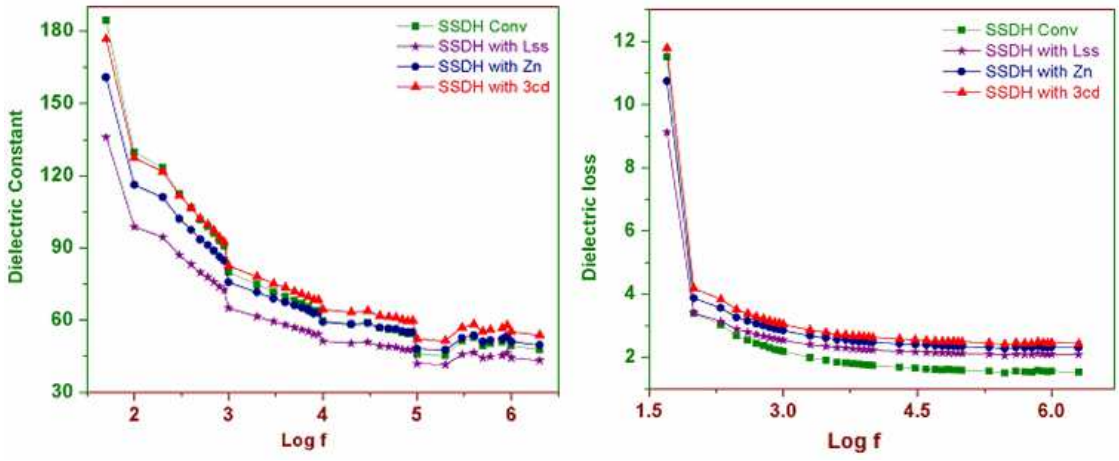

Figure1.11 Dielectric constant (vs log f) for pure and metal doped SSDH grown crystal

3.6 Etching Studies

The increasing demand for crystals of better perfection for use in the fabrication of electronic devices and in the understanding of the mechanism of plastic deformation leads to analyze the defects in crystal. Etching technique is one of the powerful tools for the observation of defects in crystals. Dislocations easily appear in the crystal especially in the initial stages of their growth [22]. The presence of dislocations in crystal are inferred from the observation of etch pits formed (Sangwal 2005).

The as grown crystals of pure and doped SSDH were subjected to chemical etching studies. Water was used as etchant since it is found to be suitable for revealing dislocations. The growth features and etch patterns were observed on the flat surface of the grown crystals. Moreover the studies were carried out at room temperature for a known duration ranging from 10 s, 15 s and 30 seconds. The surface morphology of the as grown single crystals of pure and doped SSDH is shown in Figure 1.13 a.

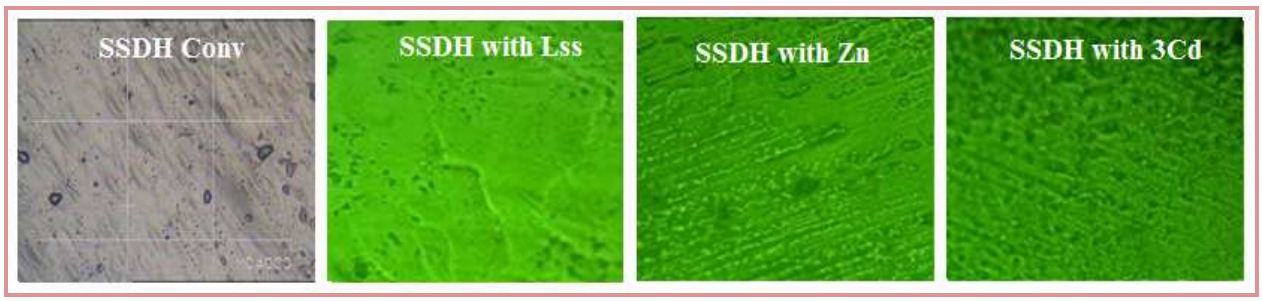

Figure 1.13(a) As grown surface of pure and doped SSDH crystal

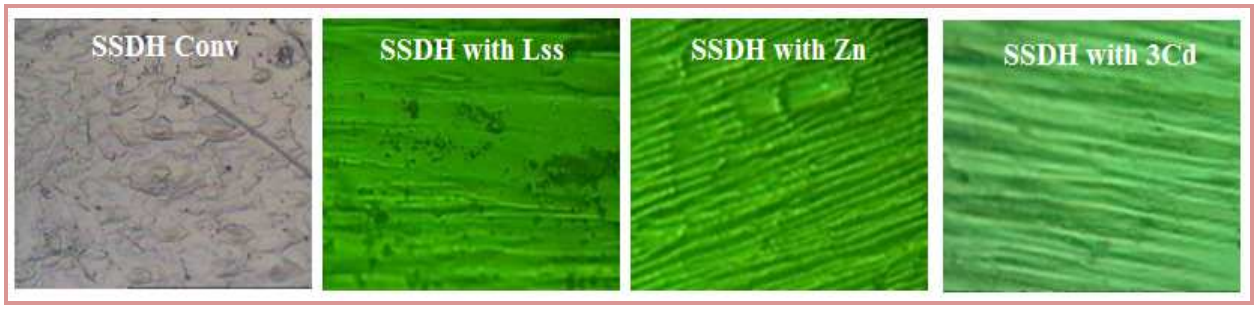

Figure 1.13(b) 10 sec, Etched surfaces of pure and doped SSDH crystal

Before etching, small etch pits are observed on the surface. The sample was then cleaned and dipped in doubly distilled water for 10, 15 and 30 seconds and dried by gently pressing between filter paper. The micro morphology was photographed and analyzed under the optical microscope. The typical etch pattern observed after etching for 10 secs in water is shown in Figure 1.13 b. The etch pits are square in shape and are aligned along the flat surface. The square pattern of the etch pits (dislocation) observed is due to the high kink nucleation. The inhibitions of the etchant were high. The kink nucleation is primarily controlled by the effective undersaturation of the dissolving crystal of the etchant. Similar etch pits with different size were observed while etching for 15 secs and 30 secs as shown in figure 1.13 (c and d). As the etching time is increased the size of the etch pits were also found to increase but the pit pattern remains the same. This shows that etch pits or the etch patterns are dislocations outcrops at the surface. The dislocations may also be due to plastic deformation caused by thermal stresses.

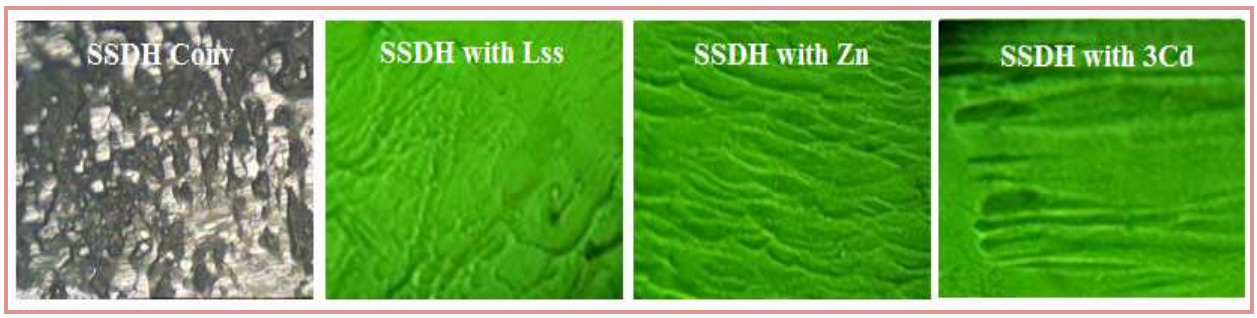

Figure 1.13(c) 15 sec, Etched surfaces of pure and doped SSDH crystal

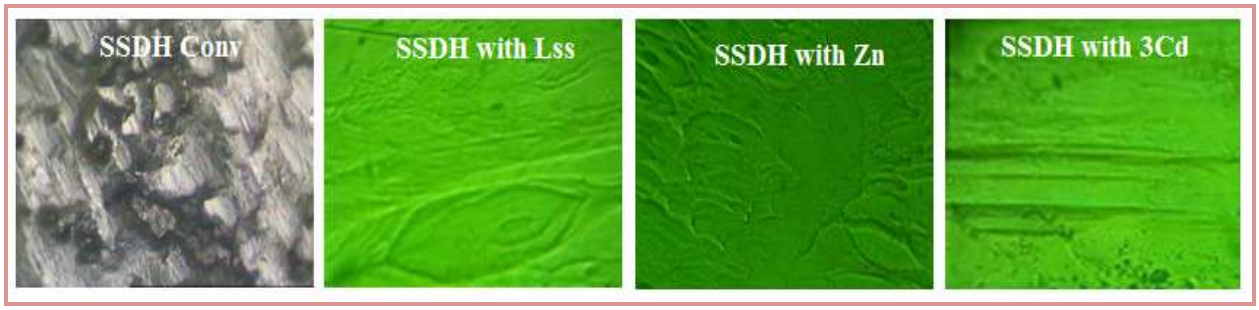

Figure 1.13(d) 30 sec, Etched surfaces of pure and doped SSDH crystal

3.7 Conclusions

Good quality single crystals of pure and metal doped SSDH were grown by slow evaporation solution growth technique. The grown crystals were optically transparent. The single crystal X-ray diffraction studies confirm that the grown crystal belongs to the orthorhombic crystal system and the powder X-ray diffraction analysis supports the good crystalline perfection of the grown crystals. The functional groups were confirmed by the FT-IR analysis.

The presence of zinc and cadmium in pure SSDH and the incorporation of zinc and cadmium ions in the doped SSDH crystals have been verified using EDAX analysis. Optical studies show that both the crystals have a wide transparency window in the entire visible regions, making it an ideal candidate for NLO applications. The dielectric studies show that the dielectric constant and dielectric loss decrease exponentially with frequency. The etching studies reveal the volume and linear defects.

References

1. W. J. Liu, C. Ferrari, M. Zha, L. Zanotti, and S. S. Jiang, Cryst. Res. Technol. 35 (2000),1215.
2. S. Dhanuskodi and K. Vasantha, Spectrochim. Acta A 61 (2005) 1777.
3. Z. G. Hu, N. Ushiyama, Y. K. Yap, M. Yoshimura, Y. Mori, and T. Sasaki, J. Cryst. Growth 654 (2002) 237-239.
4. Dennis J and Henisch H K 1967 J. Electrochem. Soc. 114, 263
5. Bohandy J and Murphy J C 1968 ActaCrystallogr. B24, 286
6. J.W. Bats, P. Coppens, Acta Crystallogr. B 31 (1975) 1467.
7. M. H. Jiang and Q. Fang.(1999). Adv. Mater. 11:1147-1151.
8. C. Razzetti, M. Ardoino, L. Zanotti, M. Zha, C. Paorici, Cryst. Res. Technol. 37 (2002) 456.
9. J.H. Westbrook, H. Report 58-RL-2033 of the G.E. Research Laboratory, USA, 1958.
10. W. Mott, Micro Indentation Hardness Testing, Butterworths, London, 1956.
11. N. Vijayan, G. Bhagavannarayana, and Alex Slawin, Mater. Lett., 62 (2008), 2480-2482.
12. A. Meijerink, G. Blasse and M. Glasbeek. (1990), J. Phys. Condens. Matter.,2 (1990), 6303-6313.

13. J.X. Wang, S.S Xie, H.J. Yuan, X.Q. Yan, D.F. Liu, Y. Gao, Z.P. Zhou, L. Song, L.F. Liu, X.W. Zhao, X.Y. Dou, W.Y. Zhou, and G. Wang, Solid State Commun. 131, (2004),435-440.
14. B.R. Lawn, E.R. Fuller, J. Mater. Sci. 9 (1975) 2016.
15. J.H. Westbrook, H. Report 58-RL-2033 of the G.E. Research Laboratory, USA, 1958.
16. K. Girija, G.R. Sivakumar, S. Narayanakalkura, P. Ramasamy, D.R. Joshi, and P.B. Sivaraman, Mater. Chem. Phys. 63 (2000) 50.
17. A.G. Kunjomana, K.A. Chandrasekaran, Cryst. Res. Technol. 40 (2005) 782.
18. B. Narasimha, R. N. Choudhary, K. V.Roa Mater. Sci. 23 (1988) 1416.
19. K. V. Rao, A. Smakula, J. Appl. Phys.36 (1965) 2031-2038.
20. U. Von Hundelshausen, Phys. Lett. 34A (1971) 405-406.
21. Christo.Balarew and Duhlev. Rumen, Journal of Solid State Chemistry, 55.1 (1984), 1-6.
22. A.A. Chernov. (1989), Contemporary Physics, 30 (1989), 251-276.
23. K.Sangwal, Cryst. Res. Technol., 40 (2005), 635-648.

*****